Effects of the concentration of solids on the phenomenon of super-elevation in artificial curved open channels

INGENIERIA CIVIL

Efectos de la concentración de sólidos en el fenómeno de sobre-elevación en canales artificiales curvos

Iván A. Guerrero§[1] David E. Villota[1], Gustavo A. Córdoba[1], Hernán J. Gómez[1]

[1] GRAMA Research Group, Universidad de Nariño, Colombia.§ ivan.guerrero-diaz@hotmail.com, devillota@hotmail.com, gcordobaguerrero@gmail.com, hgomezza@unal.edu.co

Abstract

This present study analyses the effects of the concentration of solids in the over-elevation phenomenon in a canal with a 180° curvature and a constant trapezoidal transversal section, with a firm bed, the fluid has a non-colloidal, mono-disperse distribution of relatively spherical particles of 1mm in size, thus making the rheology of the flow describable by the Einstein-Roscoe equation (1). Two stages are proposed for the development of the research; the first corresponds to physical experimentation, achieved using an artificial canal, in which 420 tests were carried out using different concentration of solids and two slopes, in order to determine the behaviour of the bi-phased flow. All of this is carried out by using experimental results and results obtained from numerical models. The data collected from the experimental process is compared to the results obtained from the theoretical models that are reported in literature. An over-elevation equation was formulated from the analysis, which can be used for the bi-phased conditions described in this article. During the second phase, numerical modelling using the TITAN2F software was carried out, where laboratory conditions are replicated. Data found from numerical modelling is compared with experimental results, with the intention of validating the numerical model that TITAN2F uses. From what is mentioned above, it was deduced that TITAN2F effectively reproduces the hydraulic phenomenon. However, it is also observed that the program has a low susceptibility to changes in the concentration of solids, due to the scale being used.

Keywords: *Curved open channels, Concentration of solids, Superelevation, Titan2F*

Resumen

En el presente estudio se analiza los efectos de la concentración de sólidos en el fenómeno de sobre-elevación en un canal con una curva de 180° y de sección transversal trapezoidal constante, con lecho fijo, el fluido tiene una distribución monodispersa no coloidal de partículas aproximadamente esféricas de tamaño 1 mm, por lo que la reología del flujo puede ser descrita por la ecuación de Einstein-Roscoe. Para el desarrollo de la investigación se plantean dos fases; la primera, correspondiente a experimentación física, por medio de un canal artificial, en el que se realizaron 420 ensayos con diferentes concentraciones de sólidos y dos pendientes, para determinar el comportamiento del flujo bifásico. Todo esto se lleva a cabo comparando resultados experimentales y con resultados obtenidos de modelos numéricos. Los datos alcanzados en el proceso experimental se comparan con los resultados obtenidos a partir de modelos teóricos reportados en la literatura. A partir del análisis realizado Se formuló una ecuación de sobre-elevación, que puede ser usada para las condiciones de flujos bifásicos expuestas en este artículo. En la segunda fase se realizan modelaciones numéricas usando el software TITAN2F, donde se replican las condiciones del laboratorio. Los datos encontrados a partir de las modelaciones numéricas se compararon con los resultados experimentales, con el fin de validar el modelo numérico que utiliza TITAN2F. De lo anterior, se pudo deducir que efectivamente, TITAN2F reproduce el fenómeno hidráulico; sin embargo, se observa que el programa tiene baja susceptibilidad a cambios de concentración de sólidos debido a la escala utilizada.

Palabras clave: *Canales curvos, Concentración de sólidos, Sobre elevación, Titan2F*

1. Introduction

Natural hydraulic behaviour is very complex, which is why theoretical simplifications that facilitate the analysis of natural channels are made in hydraulics (2). However, these simplifications eliminate characteristic that manifest themselves in real flows, such as viscosity, rotationality and compressibility. This generates uncertainty in the results, which increases when working with bi-phased flows. Taking the number of solids in a flow into account, its rheology can change drastically, changing from a Newtonian to a non-Newtonian fluid (3,4).

The problem that is approach in this investigation is related to the effects that might occur on the surface levels of water in the curving of a canal when solid particles are added in different concentrations.

Hydraulic phenomena can be analysed using analytic, numerical, and experimental models. Analytic models make approximations to the behaviour of the fluid using empirical simplifications and applicable equations for fluids without solids (5). Numerical simulation models (6,7) solve complex equation systems for the processing of data (8,9), allowing for approximations that are closer to reality. Experimental models (5,10,11), are generally smaller scale reproductions that are used to delimitate variables that intervene in a phenomenon, and can be used to obtain statistics or empirical equations that explain it (10,12).

The previously presented methods will be used in this study to analyse the effects produced by the concentration of solids in the behaviour of the phenomenon of superelevation (11,13,14). This hydraulic phenomenon presents itself in open canals with curved alignments and is characterized by an increase in the height of the flow at the external wall of the curve and a decrease at the inner curve (2). Usually, in engineering, this phenome-non is ap-proached through equations that do not take the solid phase of the flow into account (2,15). The purpose of this study is to make a contribution towards the understanding of this phenomenon, which can occur in mudflows, inundations or river floods. All of these events can pose a great threat to infrastructure and to life.

Mudflows or lahars (3,16,17), are flows with a high concentration of solids, which can range from 20% to more than 60% of the total volume of the flow (18,19,4,20). These flows do not behave as Newtonian fluids since the shear stress and the velocity gradient do not have a linear relationship. (4,21).

The purpose of this work is to make a physical and numerical investigation using an experimental model, in order to make laboratory tests in an artificial canal, controlling the percentage of solids as well as the slope at the entrance of the curve. Additionally, the work intends to make numerical simulations, using the specialised software TITAN2F (22,9), in which the initial conditions used in the laboratory are replicated, thereby obtaining results about velocity and superelevation. Finally, the results obtained from both methods are compared to an analytical mathematical model that applies the second law of Newton, and a simplification of the velocity profile of the cross section of the canal (2).

2. Methodology

2.1 Experimental model.

According to Baird (23) and Gutiérrez & Salazar (24), among others, an experimental design is defined as an application of the scientific method consolidated as a group of statistical and engineering techniques, that have been widely used in investigations with the purpose of understanding the functioning of a system or of a phenomenon.

With this in mind, a series of experiments were carried out, in which controlled changes were made in specific variables, such as the slope and the percentage of solids, in order to observe and understand the relationship between the cause and effects of these variables in the superelevation phenomenon.

A variety of studies have been made for the explaining and predicting of this phenomenon, such as (2,25,10,14), all of which have created good approximations of the event for pure fluids. These approximations generally only require geometrical and velocity parameters for their solutions, with the advantage that they only predict the maximal superelevation and it is not possible to know at what angle of the curvature it happens, like for example in equations 1, 2, and 3 (2,26).

$$\Delta h = \frac{V_z{}^2 b}{g r_c} \qquad (1)$$

Where b is the width of the canal, Vz is the velocity at the entrance of the curve. g is gravity and r_c is the radius of the curvature.

$$\Delta h = 2.30 \frac{V_z^2}{g} \log \frac{r_0}{r_i} \qquad (2)$$

Where r_0 is the external radius and r_i is the internal radius.

$$\Delta h = \frac{V_{max}^2}{g} \left[\frac{20}{3} \frac{r_c}{b} - 16 \frac{r_c^3}{b^3} + \left(\frac{4r_c^2}{b^2} - 1 \right)^2 \ln \frac{2r_c+b}{2r_c-b} \right]$$
$$(3)$$

Where *Vmax* is the maximum velocity of the cross sections before reaching the curve.

In these equations, *Δh* is the superelevation as the difference between the minimum and maximum level in a section of the curve. Out of these equation, the one that is used the most is equation 1, which can be deduced from a simple dimensional analysis.

2.1.1 Construction of the artificial canal

The canal was designed with a trapezoidal cross section measuring 0.3m and a height of 0.28m (Figure 1a) and is divided into three zones. The first zone is straight (Figure 1b). At its start, a compartment with a capacity of 50 litres was placed. This zone has a variable slope between 0% and 12.5%. The second zone is a 180° curve, as shown in (Figure 1b), with a varying bottom slope which varies along the way, which will be used in future studies. Finally, the last zone is a straight path with a constant slope at 2%, and ends in a curve that leads to a supplying tank.
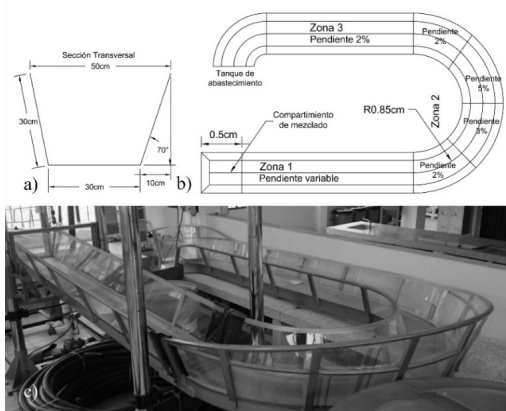

Figure 1. *a) cross section of the canal b) floor of the artificial canal c) Laboratory assembly*

2.1.2 Choice of variables.

The parameters analysed in the phenomenon being studied are: the longitudinal slope, the concentration of solids, volume, and the shape of the canal. Since the laboratory assembly has specific dimensions (Figure 1), the variables to be controlled were reduced to the slope of the canal and the concentration of solids.

2 different slopes were considered, at 5% and 10%. Likewise, taking into account that the mixing system has a maximum limit of 30% solids, the range being evaluated will be from 0% to 30% solids in volumetric percentage. By using increases of 5%, this range was divided between 7 values: 0, 5, 10, 15, 20, 25, 30 percentage of solids. However, for the analysis of the information obtained, the number of solids deposited in the first section of the straight path is taken into account.

The tests were made at a room temperature of approximately 16°C. The solid phase was made out of sand with a mean diameter of 1mm, and a density of 2.5 g/cm^3. The fluid has a monodisperse, non-colloidal distribution.

With the purpose of analysing the results from equations 1, 2, and 3, experiments were made with pure water. From these experiments, the theoretical velocity using each of the equations was deduced. Tables 1 and 2.

Table 1. *Results of theoretical velocities and experimental velocities with a 5% slope for pure water 5% superelevation of 0.176m)*

Descripción	Velocidad		% Error
Velocidad Experimental	2.200	m/s	-------------
Ecuación 1	2.210	m/s	0.53
Ecuación 2	2.200	m/s	0.06
Ecuación 3	3.020	m/s	27.20

Table 2. *Results of theoretical velocities and experimental velocity with a 10% slope for pure water (over-elevation of 0.218m)*

Descripción	Velocidad		% Error
Velocidad Experimental	2.543	m/s	-----------
Ecuación 1	2.463	m/s	3.31
Ecuación 2	2.452	m/s	3.79
Ecuación 3	3.365	m/s	24.38

Taking the results of Tables 1 and 2 into account, it was decided that equations 1 and 2 would be used, since they give results that are close to those observed in the laboratory

2.1.3 Size of the sampling

With the intention of confirming that the sample size has statistical validity, it is necessary to obtain a sample that represents it. For this end, equation 4 was used, (27,28), in which *n* is the size of the sample, *k* is the corresponding value of the Gauss distribution (28), *p* is the prevalence of the parameter to be evaluated, and *e* is the percentage of error that will be allowed. Finally, *n* was calculated for differnt conditions of the level of confidence and percentage of error allowed, from which Table 3 was obtained.

$$n = \frac{k^2 p(1-p)}{e^2} \qquad (4)$$

Table3: Number of tries depending on the level of confidence and the percentage of error allowed. (3 levels of confidence for each % of error)

Nivel De Confianza	E	K	p	1-p	n	Número Total de Ensayos
95	0.05	1.96	0.5	0.5	384	5376
90	0.05	1.65	0.5	0.5	272	3808
85	0.05	1.44	0.5	0.5	207	2898
95	0.1	1.96	0.5	0.5	96	1344
90	0.1	1.65	0.5	0.5	68	952
85	0.1	1.44	0.5	0.5	52	728
95	0.15	1.96	0.5	0.5	43	602
90	0.15	1.65	0.5	0.5	30	420
85	0.15	1.44	0.5	0.5	23	322

With the data obtained from Table 3, and considering a level of confidence of 90% and a percentage of error of 15%, a sample of 30 tries for each scenario is obtained, for a total of 420 tries.

2.1.4 Experimental procedure

In order to carry out the experiments, two video cameras were placed over the canal. The first one was placed at zone one, recording facing its bottom, where position marks were placed every 10 cm, with the intent of determining the velocity that the flow passed with at that sector. The second one was placed at zone two, facing the scales that were placed at the outer wall of the canal, in order to register the maximum height that was produced by the superelevation phenomenon.

Then, the granular material was loaded inside the initial compartment and the rest of the control volume was filled with water. After this, the mixing device was activated and the flow was released. It is worth noting that the mixing was carried out with two rotors with 800 W of potency, and the homogeneity control proved difficult.

2.2 Digital modelling with Tita2F

TITAN2F is a software developed by PhD. Gustavo Córdoba at University of Buffalo, United States, for the numerical simulation of the behaviour of bi-phased flows over a digital terrain model (22,9). TITAN2F takes the dynamics of the solid material into account through the Mohr-Coulomb model and combines it with hydraulic models by using shallow waters equations. The interaction between the two phases is determined through a semi-empirical equation that relies on the percentage of solids, (22).

The software requires the input of the initial conditions of the mud flow that is to be modelled, such as: volume, location, the digital terrain model over which the modelling will be carried out, the concentration of solids, the duration of the simulation, among other. (9).

2.2.1 Construction of the Digital Model.

The digital elevation model DEM, is a digital or computational representation usually of the geomorphology of a terrain. It is equally useful for representing the morphology of any element like streets, houses, cities and/or canals.

DEMs have been evolving in precision (29,30,31) as well as in their own generation method (32,33,34), in such a way that they allow for a great number of analysis with re-creatable, accessible, and trustworthy results (5,35).

DEMs are used in numerical modelling that is developed through software tools, as is the case of TITAN2F (9), LAHARZ (36,37), COMSOL Multiphysics, FLOW 3D (38,7), among others. It

is worth noting that with a higher resolution comes a higher computational cost of the calculations that are made through it.

The DEM was built from the dimensions of the artificial canal (Figure 1), through a three-dimensional scheme made in AutoCAD Civil 3D™ (academic version), from which a vectorial representation of the canal was obtained with a precision of 0.01m (Figure 2)
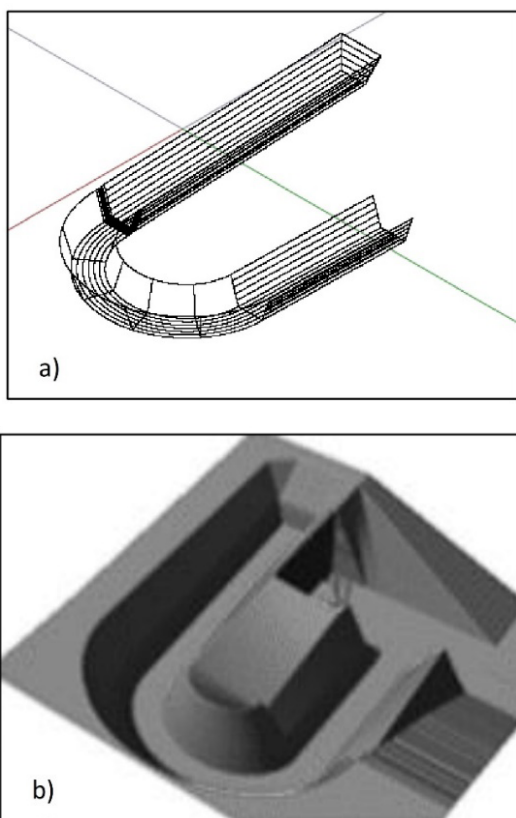

Figure 2 a) Scheme of the canal in AutoCAD Civil 3D™(academic version). b) representation of the DEM in GRASS GIS.

Once the vectorial representation is obtained, it was imported to the Geographical Information System GRASS GIS, a free use software that is compatible with TITA2F (22). Once it has been imported, we use the command r.fillnulls (39) which is part of GRASS GIS, which completes the remainder of the information through interpolations in order to generate a single surface (Figure 2).

2.2.2 Entry data.

The entry data used in order to execute the model are: the concentration of solids in a range between 5% and 30%, the location of the pile in the DEM file, the volume of the pile (40 litres) and a simulation time of 5 seconds.

When executing the TITAN2F program, a set of matrixes stored in plain text files (*.txt) was obtained. These were made out of 7 columns, which contain position at x, y, z, the thickness or height of the flow, the velocity, the concentration of solids and the dynamic pressure, respectively. Each matrix represents the flow in a specific timeframe.

2.2.3 Obtainment of results from TITAN2F Software.

The results matrixes were imported to the Geographical Information System GRASS-GIS, with which height and flow velocity data was extracted, thereby obtaining the time and coordinates of the maximum superelevation.

3. RESULTS

3.1 Experimental Results

The obtained videos were processed for the obtainment of data, extracting time differences and distance travelled from the first camera, from which the entrance velocity at the curve was deduced. The height of the superelevation was observed directly from the second camera. Also, the quantity of material that deposited itself in zone one was weighed, in order to determine the percentage of solids that reached the curve. With these results, the density of the mix, according to equation (5), was calculated. The averages and statistical analysis obtained were registered in Table 4.

$$\rho_m = \rho_f * (1 - \vartheta_s) + \rho_s * (\vartheta_s) \qquad (5)$$

In this equation ρm is the density of the mix, ρ_f is the density of the fluid, ρ_s is the density of the solid and ϑs is the volumetric percentage of solids in the mix.

Table 4 Averages of the experimental results, percentage of solids, velocity and height of the superelevation.

Canal Slope (%)	Percentage of Initial Solids (%)	Percentage of Solids at the Curve Entrance (%)	Mix Density (Kg/m³)	Velocity at Curve Entrance (m/s)	superelevation ΔH (m)
	0	0	1000.00	2.204	0.176
	5	3.4	1051.25	1.971	0.171
	10	6.9	1103.75	1.91	0.147
5	15	10.4	1156.25	1.816	0.146
	20	13.9	1208.75	1.787	0.138
	25	17.4	1261.25	1.716	0.130
	30	20.9	1313.50	1.696	0.110
	0	0	1000.00	2.543	0.218
	5	3.8	1057.32	2.378	0.205
	10	7.6	1114.02	2.289	0.193
10	15	11.3	1170.72	2.203	0.173
	20	15.1	1227.42	2.152	0.183
	25	18.9	1284.12	2.069	0.167
	30	22.7	1340.50	1.71	0.171

3.2 TITAN2F Results Prediction

When representing the velocity results at the entrance of the curve, obtained from simulations in TITAN2F (Figure 3), we can see that the results for a 5% slope, with 5% and 25% of solids, are in a range between 1.89 and 1.88 m/s. For a slope of 10% and onwards, with the same percentage of solids, the range of the velocities are between 2.36 and 2.34 m/s.

When comparing with the values obtained in the laboratory, we observed that they are close to the mean velocities observed in the laboratory. However, the velocities measured in the laboratory have a greater range. In the case of a 5% slope, this range is between 2.2 m/s and 1.71 m/s for 0% and 25% of solids respectively. For a 10% slope, the range goes from 2.54 m/s and 2.06 m/s with 0% to 25% of solids respectively.
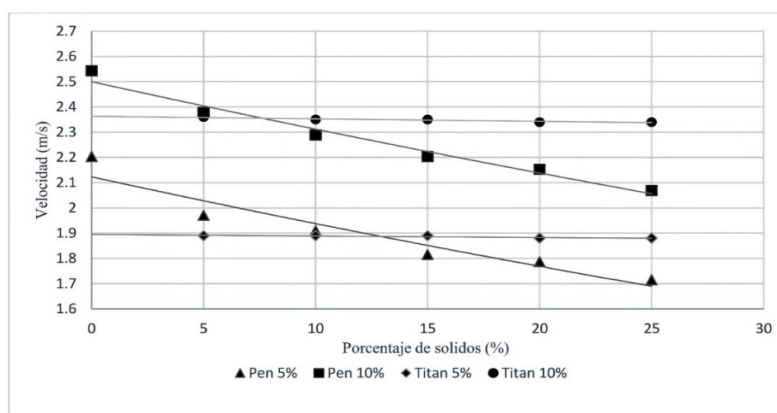

Figure 3. Comparison between experimental results of TITAN2F and experimental results of velocity vs percentage of solids.

4. DISCUSION OF RESULTS

4.1 Discussion o Experimental Results.

As it was previously mentioned, a total of 420 tests were taken, 30 for each combination of variable, slope and percentage of solids, using averages for this analysis.

When graphing experimental velocity results and superelevation for a 5% and 10% slope, an approximately linear tendency can be observed (Figure 4), with the exception of data with 30% solids, which presented errors above 10%, which is why they are excluded from later analysis.
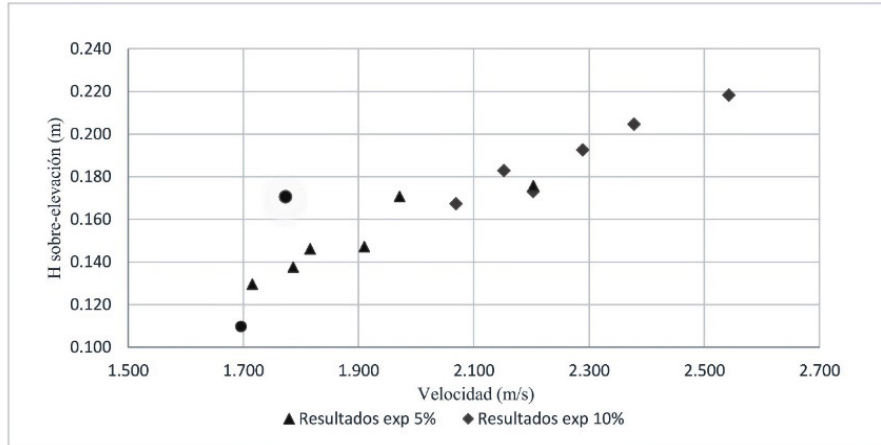

Figure 4. *Experimental velocity results versus superelevation 5% and 10% slope. The Circles represent the data excluded from later analysis.*

4.1.1 Velocity

For this analysis, we started by calculating the velocity of the flow at the entrance of the curve, using a Bernoulli approximation expressed by equation 6 (3).

$$V_b = \sqrt{2g(h_1 + sL - h_2 - h_f + \frac{V_i^2}{2g})} \qquad (6)$$

V_b is the velocity calculated at the entrance of the canal, h_1 is the height of the pile, sL is the slope of the bottom of the canal times the length of the path, h_2 is the height of the sheet at the end of the path and h_f the losses caused by friction, V_i is the initial velocity of the flow. According to the initial laboratory conditions, h_1 is 0.2 m; h_2 is equal to 2.5 cm; h_f calculated by Darcy-Weisbach (equation7) y (V_i^2) is zero.

$$hf = f * \frac{L}{4Rh} * \frac{V^2}{2g} \qquad (7)$$

Where f is the friction coefficient calculated by Colebrook-White´s (equation 8) equation, L is the distinctive characteristic of the canal and Rh is the hydraulic radio, mean velocity of the flow.

$$\frac{1}{\sqrt{f}} = \log_{10}\left(\frac{ks}{14.8Rh} + \frac{2.51}{Re\sqrt{f}}\right) \qquad (8)$$

Where ks is the rugosity coefficient, $\Re$ is Reynolds' number.

The calculating of f is carried out through an iterative process, ks is assumed as 0.0015mm for the material of the artificial canal, and $\Re$ is determined by the mean velocity of the flow in the canal.

Basing ourselves in the hypothesis that there is a direct correlation between the calculated velocity from Bernoulli and the velocity observed at the laboratory, Equation 9 is postulated.

$$V_c = K * V_b \qquad (9)$$

Where V_c is Bernoulli´s velocity, corrected so the denisity of the mix can be accounted for, and K is the factor that relates V_b and V_c. Taking into account that this factor must be equal to 1 for 0% of solids and it must diminish when increases the percentage of solids, it is assumed

that K is a function of the relationship of densities $K = f\left(\frac{\rho_f}{\rho_m}\right)$.

When graphing the velocity and the density relations, Figure 4 shows that a different behaviour for each slope exists. Using linear regression, the experimental data was adjusted to equations 10 and 11.
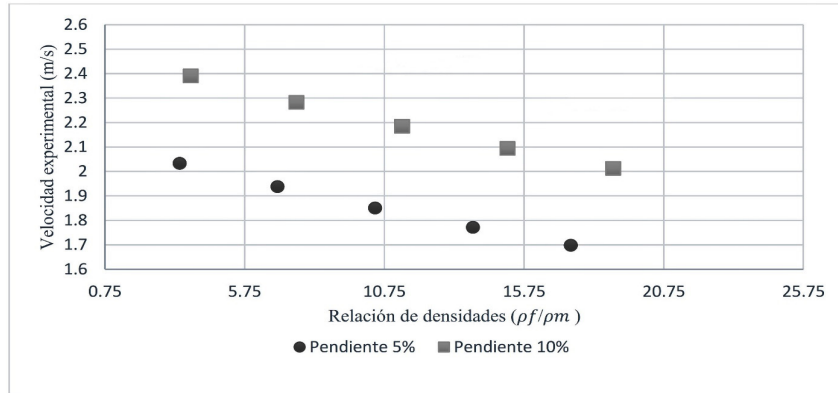
Figure 5. Relationship between velocity and the densities relation for 5 and 10 percent of slope, where (y) corresponds to the experimental velocity and (x) to the density relations.

$$V_c = 2.136 \left(\frac{\rho_f}{\rho_m}\right)^{0.987} \qquad (10)$$

$$V_c = 2.511 \left(\frac{\rho_f}{\rho_m}\right)^{0.789} \qquad (11)$$

Constants 2.136 and 2.51 of equations 10 and 11 correspond to the calculated velocities for cero percentage of solids, using Bernoulli´s equation. In order to homogenize the mathematical model, a correlation between the exponents of equations 10 and 11 is made, with the longitudinal slope of the canal, and leaving the constants as the value of the velocity obtained with Bernoulli´s approximation (equation 6), thereby obtaining equation 12.

$$V_c = V_b \left(\frac{\rho_f}{\rho_m}\right)^{1,19-0.04s} \qquad (12)$$

Where Vc is the corrected velocity. Vb is the calculated velocity of the flow, obtained from a Bernoulli´s approximation. $\left(\frac{\rho_f}{\rho_m}\right)$ is the densities relation, and s is the canal´s slope times 1.

In order to verify the level of confidence of this equation, an analysis of Pearson´s linear correlation was carried out, obtaining coefficients r5% = 0,934 for a 5% slope and r10% = 0.985 for a 10% slope as a result (40). The number of Type t5 = 5.2639 and t10 = 11.4953 Deviations was calculated for the coefficients. These results were compared to the values in Student´s Table t, with a minimum confidence level of 95% and four degrees of freedom (41), which resulted in t (0.05, 4) = 2.78. This value allows us to conclude that the results that the equation predicts and the experimental data are correlated with a level of confidence of more than 95%.

4.1.2 Superelevation

In order to simplify the analysis of superelevation, equations 1 and 2 were equalized, thereby obtaining an equation where the width of the base is in function to the curvature radiuses (equation 13). This equation represents the condition that must be met so that a single equation of superelevation in function to velocity can be obtained. In the specific case of our canal the equation is achieved with a 0.9% of error.

$$b = 2.3 \log\left(\frac{r_o}{r_i}\right) r_c \qquad (13)$$

$$\Delta h = 0.036 V^2 \qquad (14)$$

By replacing the dimensions of the canal in equations 1 and 2, an equation of superelevation in function to the velocity can be obtained, which can be applied to fluids with no solids (equation 14). In the specific case of the canal, the equation presents an error of less than 1% when checked.

Taking into account that equation 14 is useful for pure water fluids, it is necessary to make an adjustment so that bi-phased flows can be accounted for. For this end, the differences between experimental data and the results from equation 14 (Figure 6) are calculated.
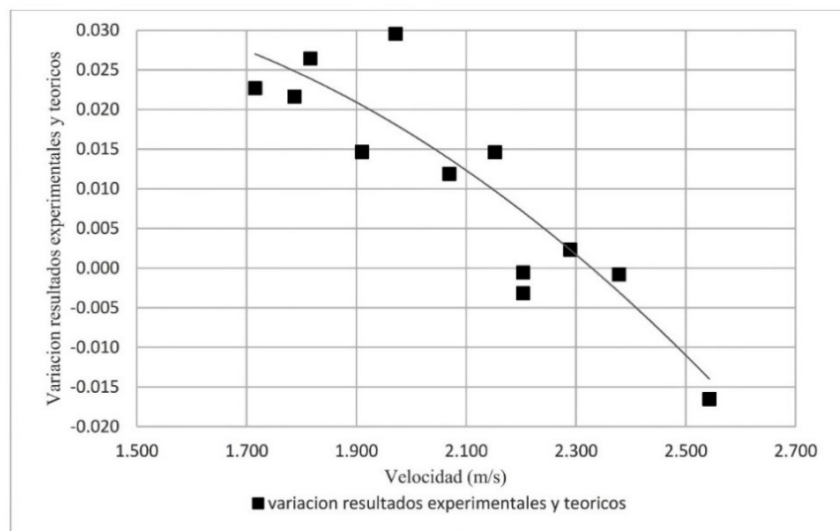

Figure 6. *Difference between experimental and theoretical results. The continuous line represents the tendency of these results.*

The difference between theoretical and experimental results on superelevation, which has been graphed above, shows a quadratic tendency, and the equation in function of the velocity (Δhc)

Was determined through minimum squares.

$$\Delta hc = -0.0257 V^2 + 0.0598 V \qquad (15)$$

Where is the difference between theoretical results (equation 14) and experimental data.

The adjustment was made by adding equations 14 and 15. Taking the analysis of velocity, (equation 12) and it resulted in a superelevation equation, in function to the corrected velocity, which takes bi-phased fluids into account (equation 16).

$$\Delta H = 0.011(V_c)^2 + 0.0598 V_c \qquad (16)$$

Where ΔH is the superelevation that takes the percentage of solids into account.

Pearson´s factors for superelevation results are r5=0.97 and r10=0.95, thus, the Type Deviations result in t5=8.1 and t10=6.1, which shows that the experimental and theoretical results (equations 16) are correlated with a level of confidence greater than 95%.

Figure 7 shows the relationship between super-elevation and the percentage of solids, where the difference between the experimental results and hydraulic theory can be appreciated. This shows that the equations for superelevation are valid for pure fluids, but they do not allow a link to the percentage of solids in the flow.
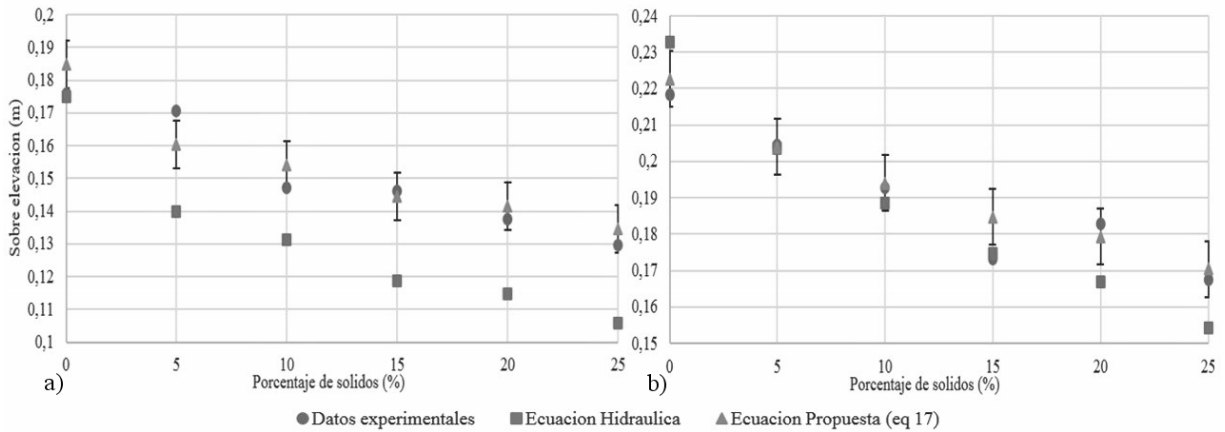
Figure 7. superelevation vs density relations a) Results for a 5% slope and b) results for a 10% slope. The triangular marks represent the proposed equation.

4.2 TITAN2F Results Discussion.

In regards to superelevation, when representing the results from TITAN2F in the GRASS GIS software (Figure 8), it can be seen how the simulation predicts a superelevation within the first 45 degrees of the curve just as it was observed experimentally. The height of the predicted for a 10% slope and 20% of solids is of 0.091m above the digital model.
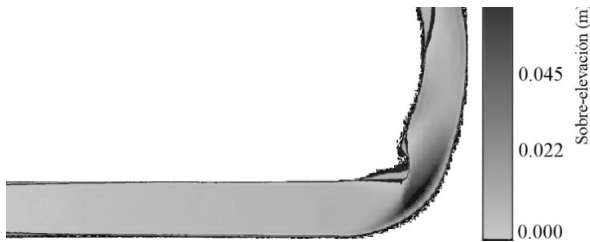

Figure 8. Ground layout representation of the GRASS GIS program in 1.3 seconds and a slope of 10% with 20% of solids.

It is important to take into account that the DEM´s resolution (1cm) and the inclination of the walls of the canal, which is 60° in relation to the horizontal, generate an uncertainty of ± 3cm vertically, which can explain part of the differences encountered.
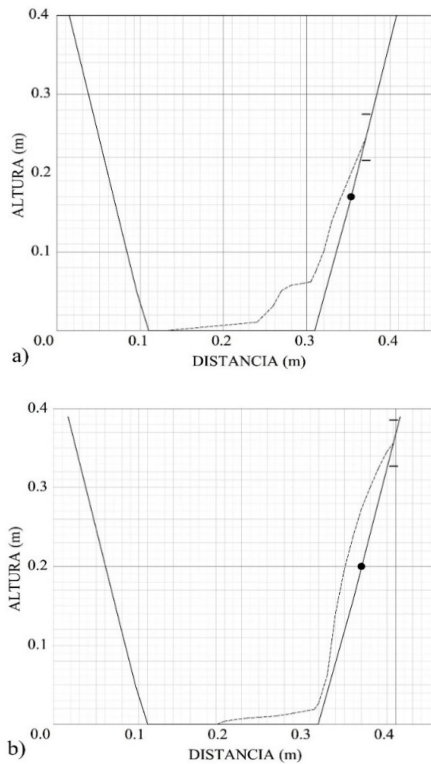

Figure 9. Comparison of the superelevation of TITAN 2F for a concentration of solids of 20% a) slope of 5% b) slope of 10%. The continuous line in a and b is the contour of the canal, the dotted line is the contour of the flow predicted by TITAN2F, the dot (•) is the superelevation measured in the laboratory and the range that has been marked at the end of the dotted line is the vertical uncertainty,

When graphing the cross sections where the simulation with TITAN2F predicts the superelevation phenomenon, it can be observed that for a 5% slope, the contour of this phenomenon is replicated by the program, as can be observed in Figure 9a. However, for a slope of 10% (Figure 9b), the contour shows a superelevation that is much bigger than the one observed in the laboratory, which allows us to conclude that when modelling in TITAN2F software, the slope has a bigger influence than the percentage of solids when defining the behaviour of the flow. When analysing superelevation results in these cross sections, an error of 28.87% and 48.85% for 5% and 10% slope, respectively, can be found. It is important to note that when increasing the slope to 10% (Figure 7b), it can be observed that the theoretical results come closer to the experimental results, based on the proposed standard deviation. However, the validity of the theoretical hydraulic equations continues to be deficient, especially for densities of over 20% of solids.

5. CONCLUSIONS

In this study, an experimental and numerical investigation for the superelevation phenomenon for the case of flows with sediments was carried out, where it was found that this phenomenon, when represented by the equations that hydraulics predicts (equations 1 and 2), shows an error of less than 5% for curve entrance velocity values between 2.0 and 2.5 m/s. When experimenting outside of this range of velocities, the percentage of error increases exponentially, which is why a correction was made in order to take the effect of the presence of sediments in the flow into account.

420 tests for 14 different scenarios were made. These tests were made with solid concentrations from 0% to 30%, with constant increases of 5%, however, it was observed that concentrations of solids greater than 25% in volume, presented a high degree of difficulty in mixing, which is why they were excluded from the analysis of results with 30% concentration of solids.

An analysis of the velocity was carried out and a new equation was formulated for the velocity of the flow. Taking the concentration of solids into account, this equation correlates the estimated velocity from

Bernoulli´s energy equation and from a relation between the density of the fluid (liquid) and the density of the bi-phased fluid. The proposed equation (Equation 12 in this text) estimates a corrected velocity, inversely correlating the concentration of solids with Bernoulli´s approximation.

During the study, it was determined that an increase in the concentration of solids in bi-phased flows diminishes superelevation when transiting through the curve. Taking the results obtained in the laboratory into account, it can be observed that superelevation values calculated by hydraulics equations stray further than one standard deviation in results with a 5% slope. The error increases when more suspended solids are found in the mix. On the other hand, when making tests with a 10% slope, results for 5% up to 15% of solids in the mix are found within a margin of error of one standard deviation; results for 0%, 20% and 25% of solids go outside the margin of error with more than one standard deviation. superelevation results show us that hydraulics equations require an adjustment in order to the into account the concentration of solids in the flow, since their margin of validity is limited to 5%, 10% and 15% of solids with a slope at the bottom of the canal of 10%.

As for the analysis of the superelevation phenomenon, we made a statistical adjustment, obtaining a semi-empirical equation (equation 16), that adjusts the current mathematical model shown in equations 1 and 2 of the text to what was observed in the laboratory. Also, it was found that this phenomenon is also correlated inversely to the percentage of solids and is correlated directly to the velocity of the flow. It is important to mention that equation 16 is valid if the curve complies with the geometrical relation shown in this article (equation 13).

In order to verify the proposed mathematical model in this study, which is represented by velocity and superelevation equations, adjusted to bi-phased flows (equations 12 and 16), it was validated with Pearson's lineal correlation method, from which confidence levels greater than 95% were obtained.

When carrying out a numerical modelling of the superelevation phenomenon with the experimentally

analysed scenarios, it was observed that TITAN2F software generates the superelevation of the flow in the outer wall of the canal´s curve in the same way it was perceived experimentally. However, when a more detailed analysis was carried out, it was observed that the program shows low susceptibility to the increase in percentage of solids, in both velocities and superelevation. Also, it was found that superelevation shows a variation of 67%, which could be considered excessive with regards to the change in the slope.

Using the current version of TITAN2F and DEM software with a resolution of 1cm, a low susceptibility was observed for the increase of the percentage of solids. This is due to the fact that the program internally rounds the calculation values to one tenth of a millimetre, due to numerical requirements. This can mean that very small or very low-resolution canals are at the edge of the programs limit. In the same, the current DEM generate an uncertainty of 3cm in the contiguous pixels of the canal walls, which can generate an error that is prolonged by rounding along the canal.

It should be noted that the results of this investigation are valid for prismatic canals, with surface conditions that are approximately smooth and with a curvature of 180°. Future investigations can be used in order to broaden and generalize results.

6. BIBLIOGRAPHY

1. Roscoe R. The viscosity of suspensions of rigid spheres. British Journal of Applied Physics. 1952; 3: p. 267–269.

2. Chow VT. Open channel hydraulics: Mac Graw Hill; 1959.

3. Streeter VL, Wylie EB, Bedford KW. Mecánica de los fluidos.: McGrawHill; 1988.

4. Chanson H. Hidraulica del Flujo en Canales Abiertos: MC. GRAW HILL.; 2002.

5. Kofman H. Modelos y simulaciones computacionales en la enseñanza de la Física. Revista educación en física. 2000; 6: p. 13-22.

6. Carrillo S JM, Castillo ELG. Análisis del flujo turbulento y bifásico en un aliviadero de presa mediante simulación numérica tridimensional. Jornadas de introducción a la investigación de la UPCT. 2010; 3: 99-101.

7. In Jornadas de introducción a la investigación de la UPCT; 2010. p. 99-101.

8. Ruiz CMX, Narváez HMB,. Implementación del programa FLOW 3D para la simulación tridimensional del flujo en una estructura de separación de caudales. Tesis pregrado, Facultad de Ingenieria Civil y Ambiental, Escuela Politecnica Nacional. Quito, Ecuador; 2015.

9. Betancur T, Palacio C. La modelación numérica como herramienta para la exploración hidrogeológica y construcción de modelos conceptuales (caso de aplicación: bajo cauca antioqueño). Dyna. 2009; 76(160): p. 39-49.

10. Córdoba G, Villarosa G, Sheridan MF, Viramonte JG, Beigt D, Salmuni G. Secondary lahar hazard assessment for Villa la Angostura, Argentina, using two-phase-titan modelling code during 2011 Cordón Caulle eruption. Nat Hazards Earth Syst Sci. 2015;15(4):757-66.

11. Ghahfarokhi GS, Vrijling PVGJ. Evaluation of Superelevation in Open Channel Bends with Probabilistic Analysis Methods. In In World Environmental and Water Resources Congress; 2008: ASCE. p. 1-14.

12. Roche O, Montserrat S, Niño Y, Tamburrino A. Experimental observations of water-like behavior of initially fluidized, dam break granular flows and their relevance for the propagation of ash-rich pyroclastic flows, J Geophys Res. 2008; 113: B12203; doi: HYPERLINK "http://dx.doi.org/10.1029/2008JB005664"\t"_blank"\o"Link to external resource: 10.1029/2008JB005664" 10.1029/2008JB005664

13. Campos-Aranda D. Aproximación empírica a la solución bivariada de avenidas de diseño en embalses sin hidrometría. Agrociencia. 2010; 44(7): p. 735-752.

14. Sánchez JMC, Elsitdié LGC. Validación de simulaciones de flujo bifásico en programas de CFD. Anuario de Jóvenes Investigadores. 2014; 7: p. 102-104.

15. Scheidl C, McArdell BW, Rickenmann D. Debris-flow velocities and superelevation in a curved laboratory channel. Canadian Geotechnical Journal. 2014; 52(3): p. 305-317.

16. Mendez D, Steeven A, Tarquino C, Candia G, Angel J. Instalación y montaje del laboratorio de hidráulica de canales. Informe de Grado. GIRARDOT: UNIMINUTO; 2009.

17. Iverson RM. The physics of debris flows. Reviews of geophysics. 1997 august; 35(3): p. 245-296.

18. Rickenmann D. Empirical relationships for debris flows. Natural hazards. 1999; 19(1): p. 47-77.

19. Coussot P, Meunier M. Recognition, classification and mechanical description of debris flows. Earth-Science Reviews. 1996; 40(3).

20. Pierson T. Hydrologic consequences of hot-rock/snowpack interactions at Mount St. Helens Volcano. Washington, 1982-84. U.S. Geological Survey ; Information Services [distributor]. 1997;: p. 39-49.

21. Pierson T. Debris-flow Hazards and Related Phenomena: Springer Berlin Heidelberg; 2005.

22. Turnbull B, Bowman ET, McElwaine JN. Debris flows: Experiments and modelling. Comptes Rendus Physique. 2015; 16(1): p. 86-96.

23. Córdoba G, Sheridan MF, Pitman EB. A two phase, depth averaged model for geophysical mass flows in the TITAN code framework. In CMG-IUGG; 2010; Pissa, Italy.

24. Baird DC. Experimentación: una introducción a la teoría de mediciones y al diseño de experimentos Mexico.D.F.: Prentice-Hall Hispanoamericana.; 1991.

25. Gutiérrez H, Salazar R. Análisis y diseño de experimentos Mexico D.F.: Mc Graw Hill; 2008.

26. Tarrab L, Vionnet CA, Rodríguez A. ANÁLISIS DE LA RELACIÓN DE ASPECTO ANCHO/TIRANTE (B/H) EN LOS FLUJOS EN CURVA. Centro de Estudios Hidro-Ambientales–CENEHA. Argentina. 2006.

27. McClung DM. Superelevation of flowing avalanches around curved channel bends. Journal of Geophysical Research. 2001; 106(B8): p. 16489-16498.

28. Ruiz-Bueno A. La mostra: alguns elements per a la seva confecció.REIRE. Revista d'Innovació i Recerca en Educació,. 2008; 1(1): p. 75-88.

29. Stephens MR, Spiegel L. Estadística. 4th ed. D.F.: Mc Graw-Hill.; 2009.

30. Broquetas A. Obtención de modelos digi-tales del terreno y detección de pequeños movimientos de la superficie terrestre mediante interferometría radar desde satélite. In AET 1997. In Teledetección aplicada a la gestión de recursos naturales y medio litoral marino: VII Congreso Nacional de Teledetección; 1997; Santiago de Compostela. p. 252-255.

31. Recondo C, Menéndez C, García P, González R, Sáez E. Estudio de las zonas propensas a sufrir deslizamientos en los Concejos de Oviedo y Mieres (Asturias) a partir de una imagen Landsat-TM y de un Modelo Digital de Elevaciones. Revista de teledetección. 2000; 14.

32. Rabus B, Eineder M, Roth A, Bamler R. The shuttle radar topography mission—a new class of digital elevation models acquired by spaceborne radar. ISPRS journal of photogrammetry and remote sensing. 2003; 57(4): p. 241-262.

33. Polidori L. Aptitudes et limitations du radar à ouverture synthétique pour la cartographie. Bulletin-Société française de photogrammétrie et de télédétection. 1992;(125).

34. Felicísimo A. Modelos Digitales de Terreno. Introducción y aplicación en las ciencias ambientales Oviedo: Extraído de http://etsimo. uniovi. es/feli; 1994.

35. Gutiérrez Á, Schnabel S, Conoscenti C, Almaru N, Ferro V, Di Stefano C, et al. Elaboración de modelos 3D de diferentes morfologías y escalas utilizando técnicas Structure-from-Motion y fotografías terrestres. Cuaternario y Geomorfología. 2016; 30(1-2): p. 23-35.

36. Frau CM, Pino LM, Rojas YO, Hernándes YM. Generalizacíon de Modelo Digital de Elevación

Condicionada por Puntos Críticos de Terreno. Bol. Ciênc. Geod. 2011; 17(3): p. 439-457.

37. Iverson RM, Schilling SP, Vallance JW. Objective delineation of lahar-inundation hazard zones. Geological Society of America Bulletin. 1998; 110(8): p. 972-984.

38. Muñoz E, Castillo M, Manea V, Manea M, Palacios D. Lahar flow simulations using LAHARZ program: Application for the Popocatépetl. Journal of Volcanology and Geothermal Research. 2009; 182: p. 13-22.

39. Li Q, Ito K, Wu Z, Lowry C, Loheide S. COMSOL Multiphysics: A Novel Approach. GROUND WATER. 2009; 47(4).

40. Neteler M, Mitasova H. Open source GIS: a GRASS GIS approach: Springer Science & Business Media; 2013.

41. Dagnino J. Coeficiente De Correlacion Lineal De Pearson. Chil Anest. 2014; 43: p. 150-153.

42. Chao L, Castaño J. Estadística para las ciencias administrativas: McGraw-Hill; 1993.